

Sampling variability under extreme skewness: sample size guidance for future methane measurement campaigns

William S. Daniels^{*,†,‡} and Dorit M. Hammerling^{†,¶}

**Department of Applied Mathematics and Statistics, Colorado School of Mines,
Golden, Colorado 80401, United States*

*†Current Affiliation: Department of Environmental Health and Engineering, Johns Hopkins
University, Baltimore, Maryland 21218, United States*

*¶Energy Emissions Modeling and Data Lab, The University of Texas at Austin,
Austin, Texas 78712, United States*

* E-mail: wdanie16@jh.edu

Abstract

Methane emissions from the oil and gas sector follow highly right-skewed distributions, making it hard to accurately quantify average emissions with a limited number of measurements. In this study, we probe the statistical implications of sampling (i.e., measuring) from these highly right-skewed distributions, using six US oil and gas basins as an example. For each basin, we provide a minimum sample size that bounds error in the average emission rate estimate introduced by sampling variability. We find that the largest emissions drive sample behavior, and by extension, sample size requirements; samples will underestimate (overestimate) average emissions if super-emitters are observed below (above) their true frequency. Importantly, we show that very large sample sizes can be necessary to mitigate this sampling effect. Furthermore, we find

12 that a one-size-fits-all sampling strategy across basins is suboptimal; differences in
13 super-emitter characteristics between basins necessitate a more tailored sampling ap-
14 proach. To increase the practical applicability of this study, we provide a web tool that
15 both reproduces our findings and performs the same analysis on any user-uploaded dis-
16 tribution of emission rates; the flexibility of this tool enables highly targeted sample
17 size guidance. This work has broad utility across fields where samples are taken from
18 right-skewed distributions.

19 Introduction

20 Methane is a potent greenhouse gas with a relatively short lifetime in the atmosphere;¹
21 this makes reducing methane emissions a key component of short-term climate action.^{2,3}
22 The oil and gas sector accounts for 21% of global anthropogenic methane emissions⁴ and
23 is viewed as a tractable opportunity for emission reduction.⁵ Methane emissions represent
24 a loss of product for many oil and gas operators, providing an economic motivation for
25 emission reduction. Furthermore, certain emission sources within the oil and gas supply
26 chain have clear mitigation pathways: emissions from malfunctioning equipment can often be
27 eliminated once the leaks are identified and engineering improvements can reduce emissions
28 from normally operating equipment like pneumatic controllers.⁵

29 Traditional activity-based, bottom-up estimates of methane emissions from the oil and
30 gas sector are known to underestimate total emissions.^{6–10} As such, efforts to reduce oil and
31 gas methane emissions increasingly rely on direct measurements from ground-based, aerial,
32 or satellite platforms.¹¹ One such effort is the creation of measurement-based emissions in-
33 ventories, in which direct measurements are used to estimate, e.g., annual total emissions
34 from a given oil and gas basin.¹² However, due to the distributed nature of oil and gas in-
35 frastructure, it is extremely challenging to measure methane at all possible source locations
36 within a basin continuously throughout the year; in practice, any measurement-based inven-
37 tory of methane emissions is created using a sample of measurements that lacks complete

38 coverage in time or across sites (or both). As such, total emissions are often estimated by
39 extrapolating an average emission rate from a limited sample of measurements (the “sample
40 mean”) to the temporal and spatial scale of the measurement-based inventory.¹³ This extrap-
41 olation introduces uncertainty in the inventory, raising a key question for future measurement
42 campaigns: how large of a sample is necessary to keep error in the sample mean introduced
43 by sampling variability below an acceptable threshold? In other words, how many sites in a
44 basin must be measured to obtain an accurate measurement-based inventory for that basin?

45 Determining an appropriate sample size is complicated by the fact that methane emissions
46 from the oil and gas sector follow highly right-skewed distributions. In particular, we know
47 from previous campaigns that methane emissions at a single point in time (e.g., from an aerial
48 or satellite technology) across many sites follow a right-skewed distribution.^{10,14–18} This is
49 likely because methane emissions over time on individual sites also follow a right-skewed
50 distribution.^{19–22} The difference between measurements over time on a single site and at a
51 single point in time over many sites is irrelevant for sample statistics (e.g., the sample mean)
52 if methane emissions follow an ergodic process.¹² However, no study (to our knowledge) has
53 tested this assumption, as doing so requires dense coverage both in time and across sites. We
54 do not test the ergodic assumption in this paper and instead illustrate findings that apply
55 to both samples over time on a single site (e.g., from continuous monitoring systems) and
56 samples at a single point in time over many sites (e.g., from an aerial or satellite technology).

57 Importantly, samples from right-skewed distributions do not behave in the same way as
58 samples from distributions with minimal skew. Principle among these differences is the rate
59 at which the sample mean converges to a normal distribution, a property guaranteed by the
60 central limit theorem. In the absence of skew, the distribution of sample means (i.e., the
61 distribution obtained by taking the mean of many repeated samples) is approximately normal
62 even if the sample size is small.²³ If the underlying distribution is skewed, however, then a
63 much larger sample size is necessary for the sample mean to approximately follow a normal
64 distribution.²⁴ In fact, the Berry–Esseen theorem states that the rate of this convergence is

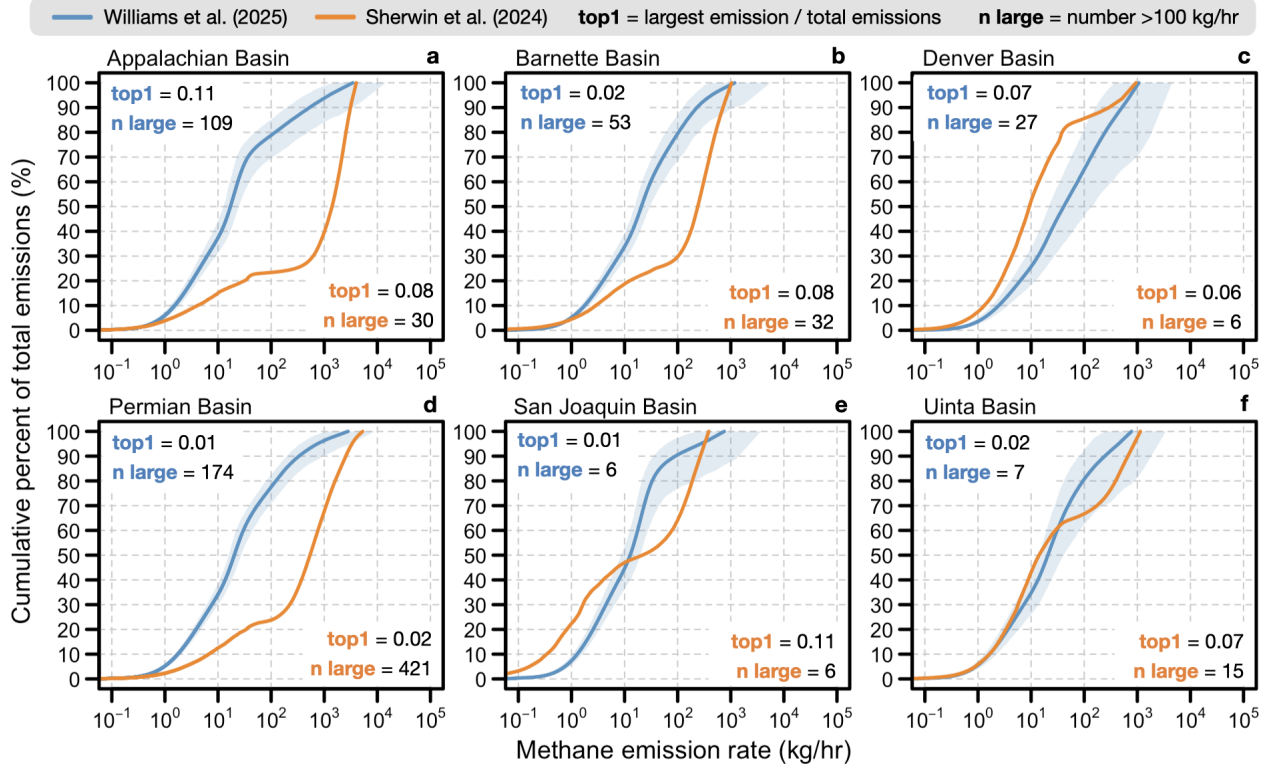


Figure 1: (a) thru (f) The basin-level emission rate distributions used in this study. Williams et al.²⁶ provide 500 realizations of each distribution; the inner 95% of these realizations is plotted as a shaded region and the average as a solid line. Sherwin et al.¹⁰ provide multiple distributions for each basin that each correspond to a separate measurement campaign; the campaign that most closely aligns in time with the Williams et al.²⁶ distribution is selected for use in this study. See the Supporting Information file for details. Two metrics related to the largest emissions are shown for each reference distribution; “top1”: the magnitude of the largest emission relative to the sum of all emissions (“total emissions”), and “n large”: the number of super-emitters (emissions >100 kg/hr).

65 a direct function of skewness.²⁵ As a result, many common practices that assume normality
66 of the sample mean cannot be used when analyzing highly right-skewed methane emissions;
67 doing so may misrepresent average emissions or underestimate uncertainty.¹⁷

68 In this article, we quantify some of the statistical implications of sampling from highly
69 right-skewed methane emission rate distributions. We then provide basin-specific sample
70 size guidance for future methane measurement campaigns that bounds error in the sample
71 mean caused by sampling variability. We conduct this analysis for six United States oil
72 and gas basins by taking many repeated samples from two state-of-the-art emission rate

73 distributions: Williams et al.²⁶ and Sherwin et al.¹⁰. These distributions are shown in
74 Figure 1. The basin-level data provided by these studies allow for basin-specific sample
75 size guidance, expanding previous analysis in Brandt et al.¹⁷. Additionally, using both sets
76 of reference distributions provides a novel comparison of these contemporary estimates of
77 methane emissions from the US oil and gas sector.^{10,26} Finally, we provide a user-friendly
78 web tool that performs the resampling analysis from this paper. This tool can be used to
79 both reproduce our findings using the Williams et al.²⁶ and Sherwin et al.¹⁰ distributions
80 and to conduct the same analysis on any user-uploaded distribution of emission rates or on a
81 selection of parametric distributions. Using this tool, our sample size guidance can be made
82 more specific to a subregion or collection of sites where users have information a priori about
83 the distribution of emission rates.

84 Results

85 Behavior of the sample mean under extreme skewness

86 Figure 2a illustrates a defining feature of highly right-skewed emission rate distributions:
87 small samples that include rare, extremely large emissions will substantially overestimate
88 the true population mean, while the majority of samples that do not contain these large
89 emissions will slightly underestimate. Figure 2a shows the emission rate distribution from
90 Sherwin et al.¹⁰ for the Denver-Julesburg basin ($n = 7,000$) and three samples of size $n =$
91 200 taken without replacement. This distribution is used for illustrative purposes in Figure
92 2; basin-specific sample size guidance is provided later in this section. In Figure 2a, Sample
93 2 includes the largest emission in the population distribution (942 kg/hr) and its mean
94 consequently overestimates the true mean by an order of magnitude. This is because Sample
95 2 is not large enough to contain a sufficient number of small emissions to average out the
96 influence of the largest emission. Samples 1 and 3 do not include the largest emissions and,
97 as a result, underestimate the true average emission rate.

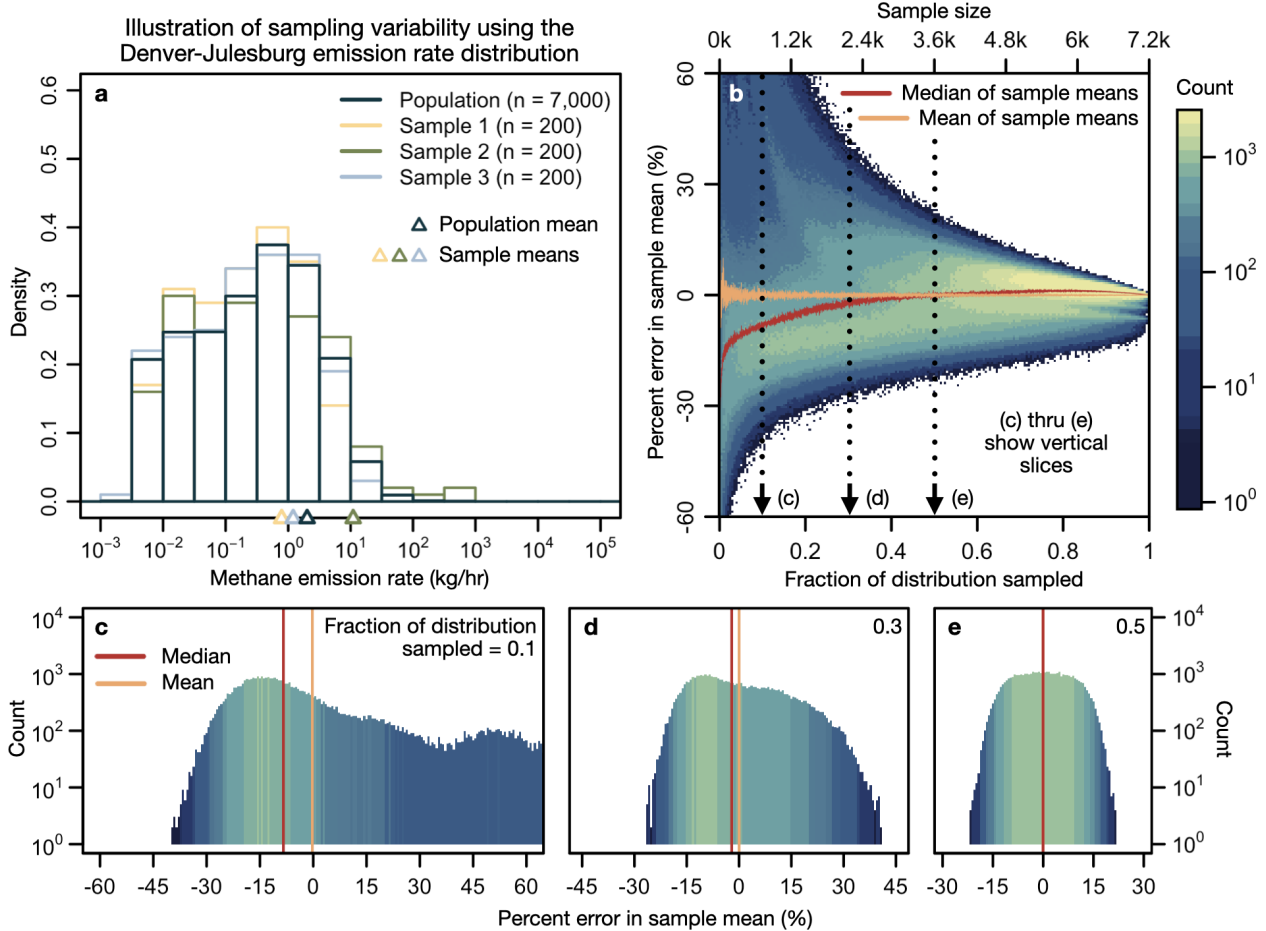


Figure 2: Illustration of sampling variability using the Denver-Julesburg emission rate distribution from Sherwin et al.²⁷. (a) Population distribution and three samples of size $n = 200$ plotted on a log-scale. Average values are shown as triangles along the horizontal axis. (b) Distribution of 1,000 repeated sample means (shown as percent errors) at sample sizes ranging from one to the length of the population distribution. The bottom axis shows sample size as a fraction of the length of the distribution, and the top axis shows sample size as a number of measurements. The color scale shows the number of samples within each grid cell. (c) thru (e) Three vertical “slices” from (b) at different sample sizes (equivalently, different sampled fractions). Both vertical axis and color scale show the number of samples within each percent error bin. Note that the mean and median are visually the same in (e).

98 Figure 2b shows the behavior of 1,000 samples taken at sample sizes ranging from a
99 single measurement to the size of the full distribution. These samples were again taken
100 without replacement; see the Methods section for a discussion of this choice. Figures 2c
101 thru e show three vertical “slices” from Figure 2b as histograms. For the Denver-Julesburg
102 basin, a surprisingly large sample is required to mitigate the influence of the rare super-

¹⁰³ emitters. Sampling 50% of the distribution (the threshold for comprehensive spatial coverage
¹⁰⁴ in Sherwin et al.¹⁰) results in a 95% confidence interval for the sample mean between -15.0%
¹⁰⁵ and 15.3% of the true mean and a maximum error of 23.0% in the sample mean. Note
¹⁰⁶ that the median becomes slightly positive when sampling over 50% of the distribution; this
¹⁰⁷ behavior is explained in the following section.

¹⁰⁸ Smaller samples amplify the effects of sampling variability: with a sample of size $n = 200$
¹⁰⁹ (as used in Figure 2a), the 95% confidence interval for the sample mean is between -40.5%
¹¹⁰ and 209.6% and the maximum error is 378.5%. Furthermore, at this sample size, there
¹¹¹ is a 72% chance that the sample mean will underestimate by failing to capture the rare,
¹¹² large emissions in the population distribution. In summary, for the Denver-Julesburg basin
¹¹³ (according to the Sherwin et al.¹⁰ distribution), measuring 200 sites results in substantial
¹¹⁴ variability in the sample mean, and even a relatively large sample covering half of the basin
¹¹⁵ is not enough to fully mitigate these sampling effects.

¹¹⁶ We pause here to highlight two important points. First, errors of the magnitude seen
¹¹⁷ in Figure 2 are not uncommon in individual emission rate estimates, regardless of the mea-
¹¹⁸ surement technology (e.g., ground-based, aerial, satellite).^{27–31} However, the percent errors
¹¹⁹ in Figure 2 are in the *mean* of many emission rate estimates, with sample sizes ranging from
¹²⁰ one to the length of the full distribution. Second, the behavior of the sample mean shown in
¹²¹ Figure 2 is not a result of *bias* in the sample mean; the sample mean is an unbiased estimator
¹²² of the population mean by definition.²³ As such, the mean of many repeated sample means
¹²³ will equal the true population mean (seen in Figure 2). However, in practice it is often
¹²⁴ infeasible to take many repeated samples, making it important to understand the behavior
¹²⁵ of an individual sample under different sample sizes and super-emitter regimes.

¹²⁶ Impact of super-emitters on sampling variability

¹²⁷ Figure 3 highlights the outsized influence of super-emitters on sampling variability. Again
¹²⁸ using the Denver-Julesburg distribution from Sherwin et al.¹⁰, Figure 3 shows three error

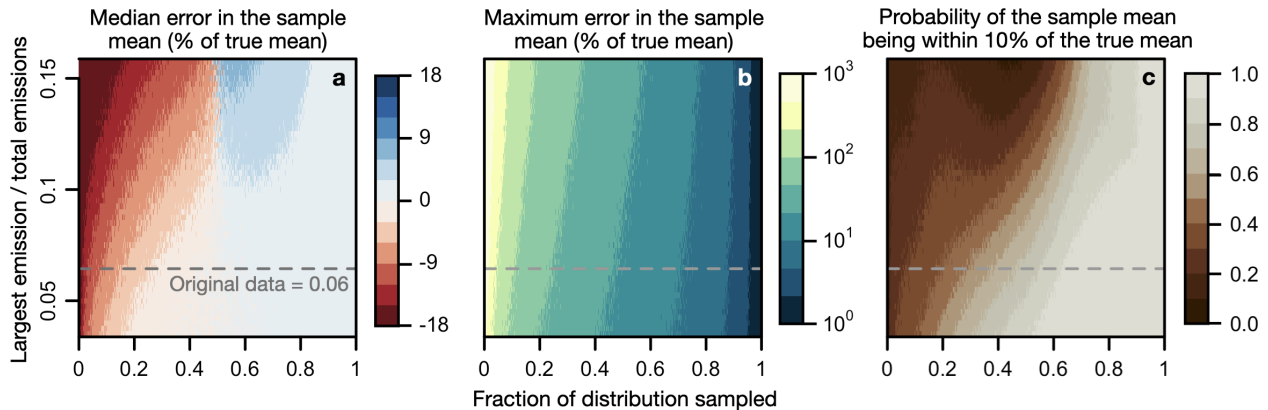


Figure 3: Impact of the largest emission in the population distribution on sampling variability. The subplots show three error metrics for the sample mean using the Denver-Julesburg emission rate distribution from Sherwin et al.¹⁰ as an example. The horizontal axis shows sample size as a fraction of the population. The vertical dimension shows how the error metrics change as the magnitude of the largest emission in the population distribution is adjusted. The vertical axis gives the magnitude of the largest emission in the population distribution relative to total emissions. The true ratio of largest emission to total emissions for the Sherwin et al.¹⁰ Denver-Julesburg basin is shown as a horizontal dashed line. All other rows are generated by artificially replacing the largest emission with a different value and taking new samples.

129 metrics for the sample mean across a range of sample sizes and as the magnitude of the
 130 largest emission in the population distribution changes. We manually adjust the largest
 131 emission in the Sherwin et al.¹⁰ distribution to illustrate this behavior.

132 At sample sizes below 50% of the distribution, the sample mean becomes more likely to
 133 underestimate as the largest emission increases (Figure 3a). This is because average (or,
 134 equivalently, cumulative) emissions are sensitive to outliers, making it increasingly necessary
 135 to observe the largest emission as its magnitude, and therefore influence on the mean, in-
 136 creases. Interestingly, sample sizes above 50% have a slight tendency to overestimate. This
 137 is because these samples are all more likely to observe the largest emission than to miss it,
 138 and once the largest emission is observed, a large number of “normal” emissions closer to the
 139 bulk of the distribution must be observed to counteract its influence.

140 A single sample becomes less likely to be within 10% of the true mean as the magnitude
 141 of the largest emission in the underlying distribution increases (Figure 3c). This metric is
 142 particularly important for determining the sample size of future measurement campaigns,

¹⁴³ as a campaign provides just one “sample” from the true emission rate distribution. As seen
¹⁴⁴ in Figure 3c, it becomes increasingly necessary to measure almost all sites within a basin as
¹⁴⁵ the magnitude of the largest emission increases relative to total emissions.

¹⁴⁶ Basin-specific sample size guidance

¹⁴⁷ Figure 4 provides sample size guidance for future methane measurement campaigns in six
¹⁴⁸ US oil and gas basins based on three error metrics related to the sample mean. For each
¹⁴⁹ metric, we show the sample size required to keep the error introduced by sampling variability
¹⁵⁰ below a given threshold. The specific thresholds shown in Figure 4 are not meant to be an
¹⁵¹ exhaustive list, rather they are meant to demonstrate how sample size requirements vary by
¹⁵² basin, reference distribution, and error tolerance.

¹⁵³ We highlight three findings from Figure 4. First, the behavior of the largest emissions
¹⁵⁴ drives sampling variability and, by extension, sample size requirements across the three
¹⁵⁵ error metrics studied here. In particular, the magnitude of the largest emission in the true
¹⁵⁶ population distribution relative to total emissions is a significant predictor ($p < 0.01$) of
¹⁵⁷ required sample size based on a simple linear regression for all three error metrics. This is a
¹⁵⁸ direct result of the behavior shown in Figure 3: the presence of super-emitters that are both
¹⁵⁹ large and rare make it hard to accurately characterize average emissions. Interestingly, basins
¹⁶⁰ with more super-emitters ($>100 \text{ kg/hr}$) require smaller samples to accurately characterize
¹⁶¹ average emissions. This is because a measurement campaign is more likely to observe super-
¹⁶² emitters in basins where they are more common, like the Permian, than in basins where they
¹⁶³ are relatively rare, like the Denver-Julesburg. As a result, it easier to characterize both the
¹⁶⁴ bulk and the tail of the emission rate distribution in the Permian, leading to a more accurate
¹⁶⁵ estimate of average emissions at smaller sample sizes. This fact has important implications
¹⁶⁶ for measurement campaign design; if the objective is to detect as many super-emitters as
¹⁶⁷ possible (e.g., for emission mitigation), then it is desirable to allocate more measurements
¹⁶⁸ to basins with more super-emitters. Conversely, if the objective is to characterize average

169 emissions as accurately as possible (e.g., for inventory development), then it is desirable to
 170 allocate more measurements to basins with fewer super-emitters where they are harder to
 171 find.

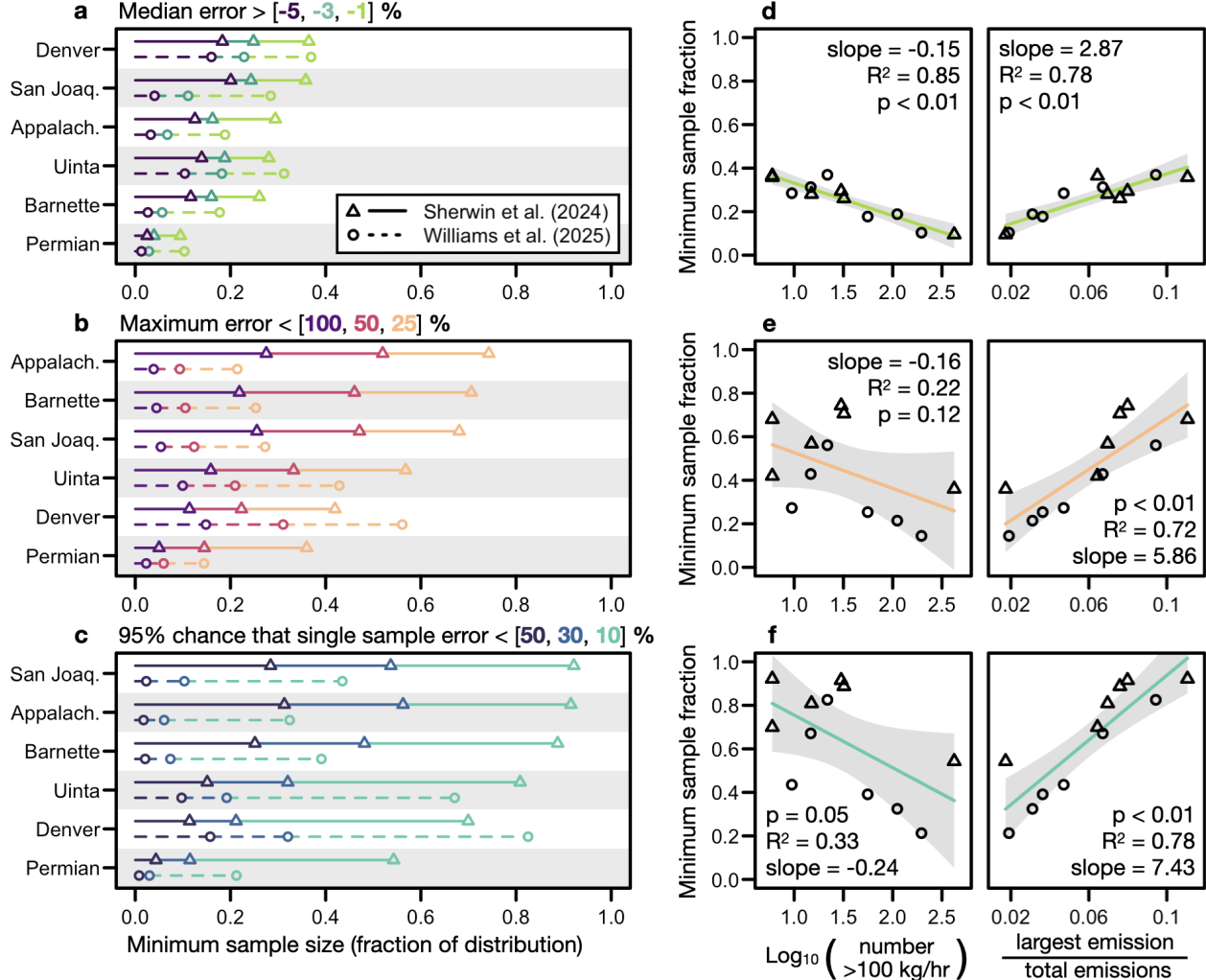


Figure 4: Basin-specific sample size guidance according to three different error metrics for the sample mean: (a) median error, (b) maximum error, and (c) single sample error. Each point shows the minimum sample size fraction required to satisfy the corresponding error threshold listed in the plot title. Correspondence between points and error thresholds is shown with color. Point and line type denote the reference distribution. Basins on the vertical axis are sorted according to the Sherwin et al.¹⁰ values within each plot. (d) thru (f) Linear relationship between two features of the emission rate distributions and the sample size required to meet the strictest error thresholds from (a) thru (c). Each point corresponds to a basin-level distribution from either Williams et al.²⁶ or Sherwin et al.¹⁰. Vertical axis shows the sample size required to satisfy the strictest error threshold from (a) thru (c), and the horizontal axes shows the feature values: the base-10 logarithm of the number of super emitters (>100 kg/hr) and the magnitude of the largest emission relative to total emissions.

172 Second, despite variability between basins, very large samples are often required to keep
173 the error in a single sample below 10% (at the 95% confidence level). As stated above,
174 this is an important metric for measurement campaign design, as each campaign provides
175 one “sample” of the emission rate distribution at a snapshot in time. For example, when
176 using the Sherwin et al.¹⁰ distributions, campaigns must measure over 80% of sites in the
177 San Joaquin, Appalachian, Barnette, and Uinta basins to keep the error in a single sample
178 below 10% (at the 95% confidence level). When using the Williams et al.²⁶ distributions,
179 campaigns must measure over 80% of sites in the Denver-Julesburg basin to meet the same
180 error threshold.

181 Third, as illustrated by the previous example, there are substantial differences between
182 the Williams et al.²⁶ and Sherwin et al.¹⁰ emission rate distributions. In particular, the
183 Williams et al.²⁶ distributions have a larger contribution from emissions <100 kg/hr than
184 the Sherwin et al.¹⁰ distributions in all but the Denver-Julesburg basin. Similarly, the
185 Sherwin et al.¹⁰ distributions have a larger contribution to total emissions from the single
186 largest emission than the Williams et al.²⁶ distributions in four of the six basins. Because
187 the largest emissions have an outsized influence on the behavior of the sample mean, the
188 Sherwin et al.¹⁰ distributions often have more variability in the sample mean than the
189 Williams et al.²⁶ distributions, which ultimately results in larger sample size requirements.
190 Given the large difference in sample size requirements between these two sets of distributions,
191 it is clear that more work is needed to definitively characterize the distribution of methane
192 emission rates in US oil and gas basins.

193 Discussion

194 Despite recent federal deregulation in the United States, ongoing efforts to measure methane
195 from the US oil and gas sector will likely continue. From an economic perspective, methane
196 emissions often represent a loss of product to oil and gas operators, incentivizing measurement-

197 based surveys to quickly identify leaks. From a reporting perspective, voluntary global pro-
198 grams, such as OGMP 2.0,³² and recent import requirements set by the European Union³³
199 both require measurement-based emissions accounting. The latter has demonstrated that
200 participation in parts of the global natural gas market may depend on the ability to measure
201 and verify emission intensities. In addition, measurement-based reporting requirements may
202 resume in the US, such as the methane fee for large release events previously introduced by
203 the US Environmental Protection Agency.³⁴

204 Whether or not they are intended to satisfy the reporting programs discussed above, all
205 future methane measurement campaigns will need to select a sample size. In this study,
206 we have provided specific sample size requirements to bound errors introduced by sampling
207 variability in six US oil and gas basins. We find that sample size requirements vary by
208 basin, largely being driven by differences in super-emitter characteristics between basins.
209 Furthermore, we find notably different sample size requirements when using different ref-
210 erence distributions.^{10,26} Improved sample size guidance will require reconciliation of these
211 state-of-the-art estimates of methane emissions from the US oil and gas sector.

212 To broaden the applicability of this work, we have created a web tool to both reproduce
213 our analysis using the Williams et al.²⁶ and Sherwin et al.¹⁰ distributions and to perform
214 the same analysis on any user-uploaded distribution or a selection of parametric distribu-
215 tions. Using this tool, sample size requirements can be made more specific to a subregion or
216 collection of sites (e.g., all sites owned by a specific operator) where users have information
217 a priori about the distribution of emission rates. Additionally, this tool can be used to cal-
218 culate sample size requirements at any user-specified error thresholds, not just the selection
219 of thresholds shown in Figure 4.

220 Our method for estimating sampling variability, made publicly available in the web tool
221 discussed above, also has broad applicability beyond methane emissions from the oil and
222 gas sector. Any measurement campaign focused on atmospheric pollutants or trace gasses
223 that is unable to visit all possible source locations will need to make a sample size deter-

²²⁴ mination. Ignoring the impact of sampling variability for any such campaign may lead to
²²⁵ misinterpretation of uncertainties in the downstream analysis.

²²⁶ While the focus of this article was on the distribution of emissions over sites at a single
²²⁷ point in time, the methodology (and web tool) are equally applicable for distributions of
²²⁸ emissions over time on a single site. In this context, a similar question often emerges:
²²⁹ how often do I need to measure a given site to accurately estimate the long-term average
²³⁰ emission rate? The answer to this question has implications for, e.g., the number of fixed
²³¹ point sensors that must be installed around the fenceline of a given facility; more sensors
²³² mean more coverage but come at a higher cost. As estimates for emission rate distributions
²³³ over time evolve (e.g., from continuous point sensors), they can be uploaded to the web tool
²³⁴ directly for temporal sample size guidance.

²³⁵ Finally, it is important to reiterate that the sample size guidance presented in this study
²³⁶ only considers sampling variability. There may be other considerations that contribute to
²³⁷ measurement campaign design, such as a desired stratification across facility types.^{12,35} Fur-
²³⁸ thermore, this study (intentionally) does not consider variability introduced by temporal
²³⁹ intermittency, or the fact that methane emissions vary over time. Other studies have made
²⁴⁰ advancements in this direction by conducting repeat measurement campaigns of the same
²⁴¹ region, finding that aggregated methane emissions are different (to varying degrees) be-
²⁴² tween repeat campaigns.^{10,35} These differences are a result of both temporal variability and
²⁴³ sampling variability (because only a subset of sites were measured). By isolating errors in
²⁴⁴ the sample mean caused solely by sampling variability, we provide a way to estimate the
²⁴⁵ contribution of temporal variability alone when conducting repeat measurement campaigns.

²⁴⁶ Methods

²⁴⁷ Reference emission rate distributions

²⁴⁸ Williams et al.²⁶ used data from 16 studies to create basin-level methane emission rate

²⁴⁹ distributions. Approximately 85% of these data are from site-level measurements using
²⁵⁰ technologies with low detection thresholds around 0.1 kg/hr, such as tracer-based releases,
²⁵¹ EPA Other Test Method (OTM 33), or Gaussian dispersion modeling. The other 15% of
²⁵² the data are from aggregated component-level measurements, such as Hi-Flow samplers or
²⁵³ flux chambers. These measurement data are scaled to the basin-level within a probabilistic
²⁵⁴ framework that leverages activity data and flaring detections.

²⁵⁵ Sherwin et al.¹⁰ used aerial data from Kairos Aerospace (now Insight M) and Carbon
²⁵⁶ Mapper (CM) together with the bottom-up simulation tool from Rutherford et al.⁸ to create
²⁵⁷ methane emission rate distributions at the basin-level. Both Kairos and CM have higher de-
²⁵⁸ tection thresholds (~ 10 kg/hr) than the measurement technologies used in Williams et al.²⁶.
²⁵⁹ Sherwin et al.¹⁰ provide multiple distributions per basin, each corresponding to a different
²⁶⁰ measurement campaign. For the analysis in this paper, we select the Sherwin et al.¹⁰ distri-
²⁶¹ butions that most closely align in time with the Williams et al.²⁶ basin-level distributions.
²⁶² See the Supporting Information file for details.

²⁶³ Resampling methodology

²⁶⁴ For both the Williams et al.²⁶ and Sherwin et al.¹⁰ emission rate distributions, we resample
²⁶⁵ the data to quantify sampling variability under different sample sizes, roughly following the
²⁶⁶ procedure in Chen et al.³⁶. That is, for each of the distributions shown in Figure 1, we
²⁶⁷ sample 1,000 times without replacement at sample sizes ranging from a single measurement
²⁶⁸ to the size of the entire distribution. We then compare the 1,000 sample means to the true
²⁶⁹ distribution mean using three metrics: the median percent error (Q_{50}), the maximum percent
²⁷⁰ error (ϵ_{\max}), and the probability of a single sample being within 10% of the truth (\mathbb{P}_{10}). For
²⁷¹ a given sample size and distribution, if we let $\bar{\mathbf{x}}^* = \{\bar{x}_1^*, \dots, \bar{x}_{1000}^*\}$ represent the 1,000 sample
²⁷² means and μ the true distribution mean, then we compute the percent error in each sample
²⁷³ mean as

$$\epsilon = 100 \times (\bar{\mathbf{x}}^* - \mu)/\mu$$

274 and the three metrics as

$$Q_{50} = \text{median}(\epsilon), \quad \epsilon_{\max} = \max(\epsilon), \quad \mathbb{P}_{10} = \frac{\text{number of } |\epsilon| < 10}{\text{length of } \epsilon}.$$

275 We sample without replacement to isolate sampling variability from other causes of variabil-
276 ity, such as temporal intermittency. The physical interpretation of this approach depends
277 on whether the true population distribution represents emissions over time on a single site
278 or emissions over sites at a single point in time. For emissions over time, sampling without
279 replacement ensures that the estimate of long-term average emissions approaches the true
280 value as measurements are taken at a higher frequency (and, in the limit, approach a truly
281 continuous measurement system). In this context, sampling 50% of the distribution can
282 be interpreted as measuring emissions half of the time. For emissions over sites, sampling
283 without replacement ensures that measuring all sites results in a correct estimate of average
284 emissions at a snapshot in time, which is the desired behavior if we ignore temporal variabil-
285 ity. In this context, sampling 50% of the distribution can be interpreted as measuring half
286 of the sites within a given domain. This paper focuses on the latter situation.

287 This resampling procedure assumes that the distributions from Williams et al.²⁶ and
288 Sherwin et al.¹⁰ are the true underlying emission distributions in their respective regions,
289 despite these distributions being (very large) samples themselves. The resampling procedure
290 also assumes that emissions of all sizes can be detected, while in reality all measurement tech-
291 nologies have a probability of detection that decreases with emission magnitude. However,
292 emissions below the detection threshold of the measurement technology can be estimated
293 (usually via a bottom-up inventory) and added to the estimate of total emissions.

294 Data Availability

295 Methane emission rate distributions from Sherwin et al.¹⁰ can be obtained from their “Source
296 data” section. Methane emission rate distributions from Williams et al.²⁶ can be obtained

²⁹⁷ from Williams³⁷.

²⁹⁸ Acknowledgments

²⁹⁹ This work was partially funded through the Energy Emissions Modeling and Data Lab
³⁰⁰ (EEMDL) and the Colorado Ongoing Basin Emissions (COBE) project.

³⁰¹ Author Contributions

³⁰² W.S.D.: Conceptualization, Analysis, Visualization, Writing - Original Draft, Writing -
³⁰³ Editing and Review. D.M.H.: Conceptualization, Writing - Editing and Review, Funding
³⁰⁴ Acquisition, Project Supervision.

³⁰⁵ Competing Interests

³⁰⁶ The authors have no competing interests to declare.

³⁰⁷ Supporting Information

- ³⁰⁸ • Supporting information file.
- ³⁰⁹ • Web tool: <https://mbasanese-sampling.share.connect.posit.cloud/>

³¹⁰ References

- ³¹¹ (1) Szopa, S.; Naik, V.; Adhikary, B.; Artaxo, P.; Berntsen, T.; Collins, W.; Fuzzi, S.; Gal-
³¹² lardo, L.; Kiendler-Scharr, A.; Klimont, Z.; Liao, H.; Unger, N.; Zanis, P. Short-Lived
³¹³ Climate Forcers. 2021; In Climate Change 2021: The Physical Science Basis. Contri-

- 314 bution of Working Group I to the Sixth Assessment Report of the Intergovernmental
315 Panel on Climate Change. <https://doi.org/10.1017/9781009157896.008>.
- 316 (2) Schleussner, C. F.; Rogelj, J.; Schaeffer, M.; Lissner, T.; Licker, R.; Fischer, E. M.;
317 Knutti, R.; Levermann, A.; Frieler, K.; Hare, W. Science and policy characteristics
318 of the Paris Agreement temperature goal. *Nature Climate Change* 2016 6:9 **2016**, 6,
319 827–835, <https://doi.org/10.1038/nclimate3096>.
- 320 (3) Collins, W. J.; Webber, C. P.; Cox, P. M.; Huntingford, C.; Lowe, J.; Sitch, S.; Chad-
321 burn, S. E.; Comyn-Platt, E.; Harper, A. B.; Hayman, G.; Powell, T. Increased im-
322 portance of methane reduction for a 1.5 degree target. *Environmental Research Letters*
323 **2018**, 13, 054003–054003, <https://doi.org/10.1088/1748-9326/AAB89C>.
- 324 (4) International Energy Agency Global Methane Tracker 2025. Paris: International Energy
325 Agency. <https://www.iea.org/reports/global-methane-tracker-2025>, 2025; CC
326 BY 4.0 License.
- 327 (5) Nisbet, E. G. et al. Methane Mitigation: Methods to Reduce Emissions, on the Path
328 to the Paris Agreement. *Reviews of Geophysics* **2020**, 58, e2019RG000675, <https://doi.org/110.1029/2019RG000675>.
- 330 (6) Alvarez, R. A. et al. Assessment of methane emissions from the U.S. oil and gas supply
331 chain. *Science* **2018**, 361, 186–188, <https://doi.org/10.1126/science.aar7204>.
- 332 (7) Chan, E.; Worthy, D. E. J.; Chan, D.; Ishizawa, M.; Moran, M. D.; Delcloo, A.; Vogel, F.
333 Eight-Year Estimates of Methane Emissions from Oil and Gas Operations in Western
334 Canada Are Nearly Twice Those Reported in Inventories. *Environmental Science &*
335 *Technology* **2020**, 54, 14899–14909, <https://doi.org/10.1021/acs.est.0c04117>.
- 336 (8) Rutherford, J. S.; Sherwin, E. D.; Ravikumar, A. P.; Heath, G. A.; Englander, J.;
337 Cooley, D.; Lyon, D.; Omara, M.; Langfitt, Q.; Brandt, A. R. Closing the methane gap

- 338 in US oil and natural gas production emissions inventories. *Nature Communications*
339 **2021**, *12*, 4715, <https://doi.org/10.1038/s41467-021-25017-4>.
- 340 (9) Conrad, B. M.; Tyner, D. R.; Li, H. Z.; Xie, D.; Johnson, M. R. A measurement-based
341 upstream oil and gas methane inventory for Alberta, Canada reveals higher emissions
342 and different sources than official estimates. *Communications Earth & Environment*
343 **2023**, *4*, 1–10, <https://doi.org/10.1038/s43247-023-01081-0>.
- 344 (10) Sherwin, E. D.; Rutherford, J. S.; Zhang, Z.; Chen, Y.; Wetherley, E. B.;
345 Yakovlev, P. V.; Berman, E. S. F.; Jones, B. B.; Cusworth, D. H.; Thorpe, A. K.;
346 Ayasse, A. K.; Duren, R. M.; Brandt, A. R. US oil and gas system emissions from
347 nearly one million aerial site measurements. *Nature* **2024**, *627*, 328–334, <https://doi.org/10.1038/s41586-024-07117-5>.
- 349 (11) Fox, T. A.; Barchyn, T. E.; Risk, D.; Ravikumar, A. P.; Hugenholtz, C. H. A review
350 of close-range and screening technologies for mitigating fugitive methane emissions
351 in upstream oil and gas. *Environmental Research Letters* **2019**, *14*, 053002–053002,
352 <https://doi.org/10.1088/1748-9326/AB0CC3>.
- 353 (12) Johnson, M. R.; Conrad, B. M.; Tyner, D. R. Creating measurement-based oil and gas
354 sector methane inventories using source-resolved aerial surveys. *Communications Earth
355 & Environment* **2023**, *4*, 1–9, <https://doi.org/10.1038/s43247-023-00769-7>.
- 356 (13) Fosdick, B. K.; Weller, Z.; Wong, H. X.; Corbett, A.; Roell, Y.; Martinez, E.; Berry, A.;
357 Gielczowski, N.; Hajny, K. D.; Moore, C. Extrapolation Approaches for Creating
358 Comprehensive Measurement-Based Methane Emissions Inventories. *ChemRxiv* **2025**,
359 <https://doi.org/10.31223/X5K14J>.
- 360 (14) Duren, R. M. et al. California’s methane super-emitters. *Nature* **2019**, *575*, 180–184,
361 <https://doi.org/10.1038/s41586-019-1720-3>.

- 362 (15) Frankenberg, C.; Thorpe, A. K.; Thompson, D. R.; Hulley, G.; Kort, E. A.; Vance, N.;
363 Borchardt, J.; Krings, T.; Gerilowski, K.; Sweeney, C.; Conley, S.; Bue, B. D.;
364 Aubrey, A. D.; Hook, S.; Green, R. O. Airborne methane remote measurements reveal
365 heavy-tail flux distribution in Four Corners region. *Proceedings of the National Academy*
366 *of Science* **2016**, *113*, 9734–9739, <https://doi.org/10.1073/pnas.1605617113>.
- 367 (16) Wang, J. L.; Daniels, W. S.; Hammerling, D. M.; Harrison, M.; Burmaster, K.;
368 George, F. C.; Ravikumar, A. P. Multiscale Methane Measurements at Oil and Gas
369 Facilities Reveal Necessary Frameworks for Improved Emissions Accounting. *Environmental*
370 *Science & Technology* **2022**, *56*, 14743–14752, <https://doi.org/10.1021/acs.est.2C06211>.
- 372 (17) Brandt, A. R.; Heath, G. A.; Cooley, D. Methane Leaks from Natural Gas Systems
373 Follow Extreme Distributions. *Environmental Science & Technology* **2016**, *50*, 12512–
374 12520, <https://doi.org/10.1021/acs.est.6b04303>.
- 375 (18) Cusworth, D. H.; Duren, R. M.; Thorpe, A. K.; Olson-Duvall, W.; Heckler, J.; Chap-
376 man, J. W.; Eastwood, M. L.; Helmlinger, M. C.; Green, R. O.; Asner, G. P.; Den-
377 nison, P. E.; Miller, C. E. Intermittency of Large Methane Emitters in the Per-
378 mian Basin. *Environmental Science & Technology Letters* **2021**, *8*, 567–573, <https://doi.org/10.1021/acs.estlett.1c00173>.
- 380 (19) Allen, D. T.; Cardoso-Saldaña, F. J.; Kimura, Y.; Chen, Q.; Xiang, Z.; Zimmerle, D.;
381 Bell, C.; Lute, C.; Duggan, J.; Harrison, M. A Methane Emission Estimation Tool
382 (MEET) for predictions of emissions from upstream oil and gas well sites with fine
383 scale temporal and spatial resolution: Model structure and applications. *Science of*
384 *The Total Environment* **2022**, *829*, 154277, <https://doi.org/10.1016/j.scitotenv.2022.154277>.
- 386 (20) Daniels, W. S.; Wang, J. L.; Ravikumar, A. P.; Harrison, M.; Roman-White, S. A.;

- 387 George, F. C.; Hammerling, D. M. Toward Multiscale Measurement-Informed Methane
388 Inventories: Reconciling Bottom-Up Site-Level Inventories with Top-Down Measure-
389 ments Using Continuous Monitoring Systems. *Environmental Science & Technology*
390 **2023**, *57*, 11823–11833, <https://doi.org/10.1021/acs.est.3c01121>.
- 391 (21) Khaliukova, O.; Zhu, Y.; Daniels, W. S.; Ravikumar, A. P.; Ross, G. B.; Roman-
392 White, S. A.; George, F. C.; Hammerling, D. M. Investigating Aerial Data Preanalysis
393 Schemes and Site-Level Methane Emission Aggregation Methods at Liquefied Natu-
394 ral Gas Facilities. *ACS ES&T Air* **2025**, *2*, 1009–1019, <https://doi.org/10.1021/acsestair.4c00301>.
- 395 (22) Daniels, W. S.; Kidd, S. G.; Yang, S. L.; Stokes, S.; Ravikumar, A. P.; Hamme-
396 ling, D. M. Intercomparison of Three Continuous Monitoring Systems on Operating
397 Oil and Gas Sites. *ACS ES&T Air* **2025**, *2*, 564–577, <https://doi.org/10.1021/acsestair.4c00298>.
- 398 (23) Casella, G.; Berger, R. *Statistical Inference*, 2nd ed.; Chapman and Hall/CRC: New
399 York, 2024; <https://doi.org/10.1201/9781003456285>.
- 400 (24) Hastie, T.; Tibshirani, R.; Friedman, J. *The Elements of Statistical Learning*; Springer
401 Series in Statistics; Springer: New York, NY, 2009; <https://doi.org/10.1007/978-0-387-84858-7>.
- 402 (25) Korolev, V. Y.; Shevtsova, I. G. On the Upper Bound for the Absolute Constant in the
403 Berry–Esseen Inequality. *Theory of Probability & Its Applications* **2010**, *54*, 638–658,
404 <https://doi.org/10.1137/S0040585X97984449>.
- 405 (26) Williams, J. P.; Omara, M.; Himmelberger, A.; Zavala-Araiza, D.; MacKay, K.; Ben-
406 mergui, J.; Sargent, M.; Wofsy, S. C.; Hamburg, S. P.; Gautam, R. Small emission
407 sources in aggregate disproportionately account for a large majority of total methane

- 411 emissions from the US oil and gas sector. *Atmospheric Chemistry and Physics* **2025**,
412 25, 1513–1532, <https://doi.org/10.5194/acp-25-1513-2025>.
- 413 (27) Sherwin, E. D.; El Abbadi, S. H.; Burdeau, P. M.; Zhang, Z.; Chen, Z.; Rutherford, J. S.;
414 Chen, Y.; Brandt, A. R. Single-blind test of nine methane-sensing satellite systems from
415 three continents. *Atmospheric Measurement Techniques* **2024**, 17, 765–782, <https://doi.org/10.5194/amt-17-765-2024>.
- 416
- 417 (28) Bell, C.; Ilonze, C.; Duggan, A.; Zimmerle, D. Performance of Continuous Emission
418 Monitoring Solutions under a Single-Blind Controlled Testing Protocol. *Environmental*
419 *Science & Technology* **2023**, 57, 5794–5805, <https://doi.org/10.1021/acs.est.2c09235>.
- 420
- 421 (29) Ilonze, C.; Emerson, E.; Duggan, A.; Zimmerle, D. Assessing the Progress of the Per-
422 formance of Continuous Monitoring Solutions under a Single-Blind Controlled Test-
423 ing Protocol. *Environmental Science & Technology* **2024**, 58, 10941–10955, <https://doi.org/10.1021/acs.est.4c08511>.
- 424
- 425 (30) Cheptonui, F.; Emerson, E.; Ilonze, C.; Day, R.; Levin, E.; Fleischmann, D.;
426 Brouwer, R.; Zimmerle, D. J. Assessing the performance of emerging and existing con-
427 tinuous monitoring solutions under a single-blind controlled testing protocol. *Elementa:*
428 *Science of the Anthropocene* **2025**, 13, 00020, <https://doi.org/10.1525/elementa.2025.00020>.
- 429
- 430 (31) El Abbadi, S. H.; Chen, Z.; Burdeau, P. M.; Rutherford, J. S.; Chen, Y.; Zhang, Z.;
431 Sherwin, E. D.; Brandt, A. R. Technological Maturity of Aircraft-Based Methane Sens-
432 ing for Greenhouse Gas Mitigation. *Environmental Science & Technology* **2024**, 58,
433 9591–9600, <https://doi.org/10.1021/acs.est.4c02439>.
- 434 (32) OGMP 2.0 The Oil & Gas Methane Partnership 2.0. 2024; UN Environment Programme
435 (UNEP). <https://ogmpartnership.com/>.

⁴³⁶ (33) Council of European Union Council regulation (EU) 2019/942 (COM(2021)0805 –
⁴³⁷ C9-0467/2021 – 2021/0423(COD)). 2023; https://www.europarl.europa.eu/doceo/document/TA-9-2023-0127_EN.html.

⁴³⁹ (34) U.S. Environmental Protection Agency. *Greenhouse Gas Reporting Rule: Revisions and
440 Confidentiality Determinations for Petroleum and Natural Gas Systems*; Final Rule 89
441 FR 42062, 2024; pp 42062–42327, <https://www.federalregister.gov/d/2024-08988>
442 (last accessed October 15, 2024).

⁴⁴³ (35) Donahue, C. P.; Oberoi, K.; Dillon, J.; Hengst, V.; Kennedy, B.; Kearney, W.;
444 Lennox, J.; Rehbein, E.; Sykes, R.; Dudiak, C.; Altamura, D.; Doherty, G.; Roos, P.;
445 Brasseur, J. K.; Thorpe, M. Aerial LiDAR Based, Source Resolved Methane Emissions
446 Inventory: Permian Basin Case Study for Benchmarking U.S. Emissions. *EarthArXiv*
447 **2025**, <https://doi.org/10.31223/X5S45T>.

⁴⁴⁸ (36) Chen, Y.; Sherwin, E. D.; Berman, E. S.; Jones, B. B.; Gordon, M. P.; Wetherley, E. B.;
449 Kort, E. A.; Brandt, A. R. Quantifying Regional Methane Emissions in the New Mexico
450 Permian Basin with a Comprehensive Aerial Survey. *Environmental Science & Tech-
nology* **2022**, *56*, 4317–4323, <https://doi.org/10.1021/acs.est.1c06458>.

⁴⁵² (37) Williams, J. P. Estimated basin-level individual methane emission rates for oil and
453 gas facilities from the continental United States in 2021. 2025; [https://doi.org/10.
454 5281/zenodo.16740519](https://doi.org/10.5281/zenodo.16740519).

455 TOC Graphic

456

